Phase transitions in lead-lanthanum zirconate-titanate ceramics with a Zr/Ti ratio of 92/8 and a La content of up to 1 at.%

1995 J. Phys.: Condens. Matter 7 895

(http://iopscience.iop.org/0953-8984/7/5/012)

J. Phys.: Condens. Matter 7 (1995) 895–906. Printed in the UK

Phase transitions in lead-lanthanum zirconate-titanate ceramics with a Zr/Ti ratio of 92/8 and a La content of up to 1 at.%

Z Ujma†, J Hańderek†, H Hassan‡, G E Kugel‡ and M Pawelczyk†

† Institute of Physics, University of Silesia, 40–007 Katowice, ul. Uniwersytecka 4, Poland

‡ Centre Lorraine d'Optique et Electronique des Solides, Université de Metz, 2 Belin, 570078 Metz Cédex 3, France

Received 20 September 1994

Abstract. Phase transitions and phase sequence in La-doped lead zirconate-titanate ceramics with a Zr/Ti ratio of 92/8 and La content up to 1 at.% were investigated by dielectric, pyroelectric, x-ray and Raman scattering methods. The phase sequence antiferroelectric (A_O)–low-temperature ferroelectric ($F_{R(LT)}$)–high-temperature ferroelectric ($F_{R(HT)}$)–paraelectric (P_C) was confirmed in these ceramics. The results obtained indicate the need to ascertain a precise phase diagram of PLZT materials in the range close to the phase boundary separating the A_O and F_R phases for low lanthanum contents by taking into account the occurrence of both $F_{R(LT)}$ and $F_{R(HT)}$ phases.

1. Introduction

Zr-rich lead zirconate-titanate (PZT) solid solutions have long been the subject of considerable interest owing to the feasibility of obtaining various phase transitions and phase sequences depending on the Zr/Ti ratio and the quantity of dopants such as La_2O_3 [1–7]. For these materials a subject arousing particular interest but also certain controversies is that of the reasons and consequences of a strongly diffuse phase transition observed between the antiferroelectric phase of orthorhombic symmetry (A_O) (space group, *Pbam*) and a low-temperature ferroelectric phase of rhombohedral symmetry ($F_{R(LT)}$) (space group, *R*3*c*) or a high-temperature ferroelectric phase of rhombohedral symmetry ($F_{R(HT)}$) (space group *R*3*m*). Studies on the occurrence of the $F_{R(LT)}$ and $F_{R(HT)}$ phases and the mechanism of the phase transition between them, especially as regards PZT solid solutions with Ti content from 6 to 12 at.%, have been reported in many publications [8–17]. Literature data on PLZT ceramics in this range of Ti contents and with low La concentrations are rather incomplete and some of them are sometimes contradictory [5–7, 18–22]. For instance, only Fritz and Keck [18] ascertained the occurrence of the $F_{R(LT)}$ and $F_{R(HT)}$ phases in the solid solution $(Pb_{0.97}La_{0.03})(Zr_{0.92}Ti_{0.08})O_3$, while Haertling and Land [5] and Haertling [6, 7] who constructed the well known phase diagram for PLZT materials (figure 1 which is taken from [6]) did not note the occurrence of the $F_{R(LT)}$ phase. In our recent paper [21], we showed that PLZT ceramics with a Zr/Ti ratio of 92/8 doped with 2 mol% La_2O_3 (i.e. 4 at.% La in the Pb sublattice) and denoted as PLZT-2/92/8 do not in fact exhibit the $F_{R(LT)}$–$F_{R(HT)}$ phase transition but a direct, strongly diffuse A_O–$F_{R(HT)}$ phase transition.

The principal objective of the studies reported here was to ascertain what content of La in the Pb sublattice causes disappearance of the $F_{R(LT)}$ phase. Phase transitions in the ceramics with a Zr/Ti ratio of 92/8, without and with La dopants, were investigated by

0953-8984/95/050895+12$19.50

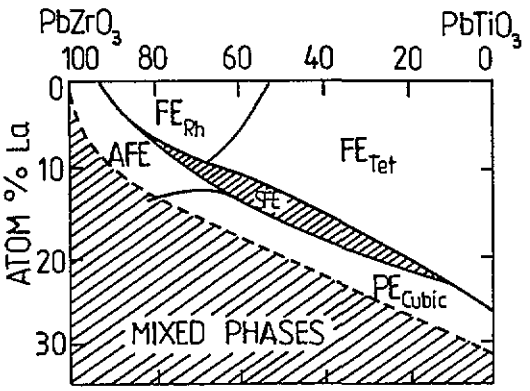

Figure 1. Room-temperature phase diagram of the PLZT system. (From [6].)

x-ray, dielectric, pyroelectric and Raman scattering measurements. Distinct indications of the $F_{R(LT)}$–$F_{R(HT)}$ phase transition were found for the tested PZT and PLZT ceramics with La dopants up to 1 at.%, contrary to results found for PLZT-92/8 + 4 at.% La [21].

2. Preparing the tested ceramics

The PZT and PLZT ceramics used for our investigations were prepared by conventional thermal synthesis of mixed oxides, described in more detail by Haertling in his review paper [6] and his monograph [7]. In all the ceramics tested, the Zr/Ti ratios were the same and equal to 92/8. In the case of the La-doped ceramics it was assumed, according to [6, 7], that in Zr-rich PLZT solid solutions the La^{3+} ions replace the Pb^{2+} ions. The required mole percentage of La_2O_3 was added to the appropriate mixture of PbO, ZrO_2 and TiO_2 with the PbO content reduced accordingly relative to the La_2O_3 content. The added quantities of the La_2O_3 correspond to 0.4 and 1 at.% La, respectively, in the Pb sublattice. The tested ceramics are further denoted as PZT-92/8, PLZT-92/8 + 0.4 at.% La and PLZT-92/8 + 1 at.% La, respectively.

The sintering processes were performed in a double crucible with a PbO atmosphere, to maintain the established composition and to reach the required densification of the ceramics. For this purpose, part of the space between the two tubular crucibles of different diameters was filled with a mixture of PbO and PbO_2, covering the sintered ceramics. The synthesis process was performed at a temperature of 1223 K for 3 h. The ceramics were then sintered successively at temperatures of 1373 and 1523 K for 3 h, after prior milling and cold pressing. The ceramics obtained were partially transparent as a result of the small size of the grains (10 μm and less) and low porosity. Owing to this latter feature, Raman scattering measurements in the 90° geometry were possible. For dielectric and pyroelectric measurements, samples of the required thickness and polished surfaces were coated with cold-deposited silver paste.

3. Dielectric and pyroelectric measurements

For measurements of the permittivity ε and dissipation factor $\tan\delta$ as a function of temperature, samples of 0.6 mm thickness were used. Measurements were performed in

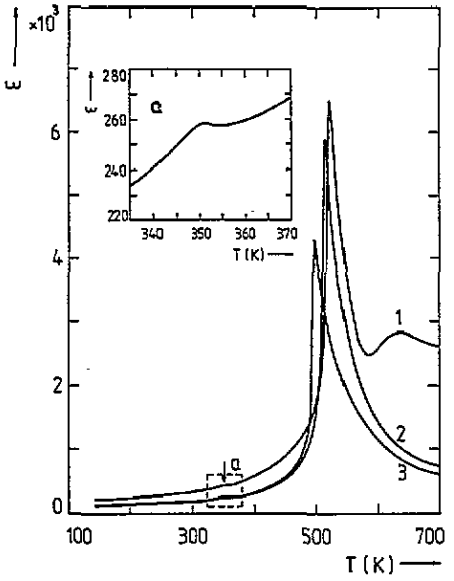

Figure 2. Permittivity versus temperature, measured on heating in a field of frequency 1 kHz, for the ceramics PZT-92/8 (curve 1), PLZT-92/8 + 0.4 at.% La (curve 2) and PLZT-92/8 + 1 at.% La (curve 3). (a) Enlargement of the $\varepsilon(T)$ curve in the vicinity of the $F_{R(LT)}$–$F_{R(HT)}$ phase transition.

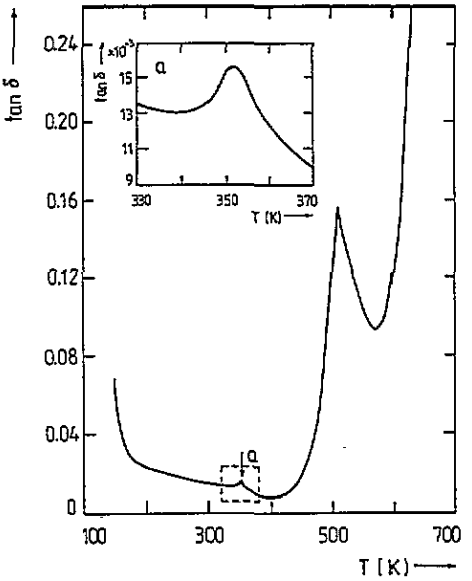

Figure 3. An example of the temperature dependence of the dissipation factor $\tan\delta$, measured on heating in a field of frequency 1 kHz, for PLZT-92/8 + 0.4 at.% La ceramics. (a) Enlargement of the $\tan\delta(T)$ curve in the vicinity of the $F_{R(LT)}$–$F_{R(HT)}$ phase transition.

a measuring field of frequency 1 kHz using a computerized automatic measuring system based on a Tesla BM-595 RLCG meter.

The $\varepsilon(T)$ curves measured on heating from about 140 to 700 K are shown in figure 2. Hunch-like anomalies in the $\varepsilon(T)$ curves, indicated by arrow a (figure 2(a)), occur at temperatures in the range from 330 to 350 K, for both PZT and PLZT ceramics. These experimental results, together with those further reported, give grounds for suggesting that these anomalies in the $\varepsilon(T)$ curves are associated with the $F_{R(LT)}$–$F_{R(HT)}$ phase transition.

Sharp maxima in the $\varepsilon(T)$ curves occur at the Curie temperatures. Both temperatures and maximum values of ε depend on the La content. For the PZT-92/8 ceramics an additional local maximum on the $\varepsilon(T)$ curve appears at temperatures $T > 600$ K, i.e. in the paraelectric phase. *In our earlier papers [19, 21] it was shown that this anomaly exhibits strong low-frequency dispersion.*

An example of the temperature dependence of $\tan\delta$ for the PLZT-92/8 + 0.4 at.% La ceramics is presented in figure 3. The $\tan\delta(T)$ curve decreases sharply on heating to about 200 K and distinct local changes can be observed in the vicinity of the $R_{R(LT)}$–$F_{R(HT)}$ phase transition. The $\tan\delta(T)$ dependences exhibit considerable deviations from normal behaviour in the vicinity of the $F_{R(HT)}$–P_C phase transition, i.e. the local maximum on the $\tan\delta(T)$ curve almost coincides with the maximum on the $\varepsilon(T)$ curve (figure 2) and its local minimum occurs at a considerably higher temperature. Behaviour of this type is characteristic of ferroelectric relaxors [23].

The temperature dependence of remanent polarization P_r was determined from hysteresis loop measurements in a field of frequency 50 Hz and strength 10–20 kV cm^{-1}. For these measurements, samples of 0.3 mm thickness were used. Curves of P_r versus temperature

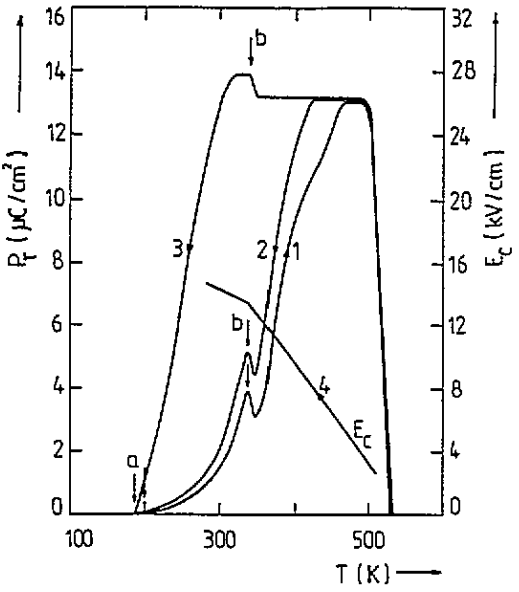

Figure 4. Remanent polarization versus temperature for PLZT-92/8 + 0.4 at.% La, measured on heating (curve 1) and cooling (curves 2 and 3) in a field of frequency 50 Hz and strength 10 kV cm^{-1} (curves 1 and 2) and 20 kV cm^{-1} (curve 3). Curve 4 is an example of coervice field as a function of temperature.

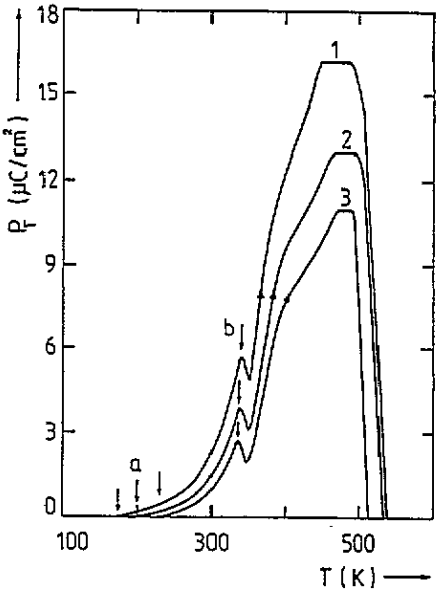

Figure 5. Remanent polarization versus temperature, measured on heating in a field of strength 10 kV cm^{-1}, for the ceramics PZT-92/8 (curve 1), PLZT-92/8 + 0.4 at.% La (curve 2) and PLZT-92/8 + 1 at.% La (curve 3).

measured in a field of strength 10 kV cm^{-1} are shown in figure 4 for heating (curve 1) and cooling (curve 2). Slim hysteresis loops were first observed starting from about 200 K (arrow a). Local maxima and minima in the $P_r(T)$ curves appear when passing the $F_{R(LT)}$–$F_{R(HT)}$ phase transition temperature (arrow b) at which weak anomalies on the $\varepsilon(T)$ and $\tan\delta(T)$ curves are found (figures 2 and 3). These local changes in the $P_r(T)$ curves differ, however, from those reported in the literature for PZT ceramics with 9 and 10 at.% Ti [4, 11]. When the strength of the measuring field is increased to 20 kV cm^{-1}, a jump-like increase in the $P_r(T)$ curve appears. This is shown in figure 4 (curve 3) in a cooling process. It is noteworthy that the temperatures of the anomalies in the $P_r(T)$ curves (arrows a and b) are independent of the strength of measuring field. The temperature at which the hysteresis loops disappear (arrow a) seems to be connected with the A_O–$F_{R(LT)}$ phase transition. In the range $T > 450$ K the strength of the measuring field had to be reduced in order to avoid breakdown of the thin ceramic samples. The $P_r(T)$ curves exhibit nearly classical (normal) behaviour in the vicinity of the $F_{R(HT)}$–P_C phase transition temperature. Figure 4 also shows the temperature dependence of the coercive field E_C (curve 4).

Because of this risk of breakdown in the high-temperature range ($T > 450$ K), for all the ceramics tested, the P_r temperature dependence was measured in a field of strength 10 kV cm^{-1} (figure 5). As may be seen, the temperature at which hysteresis loops appear (arrows a) is markedly dependent on the La content in the PLZT ceramics. Both PLZT and PZT ceramics show anomalies in the $P_r(T)$ curves (arrows b) in the vicinity of the $F_{R(LT)}$–$F_{R(HT)}$ phase transition temperatures (330–350 K), these anomalies being less dependent on the La content. As previously mentioned, when the strength of the measuring field was increased to 20 kV cm^{-1}, these anomalies change to a jump-like decrease in P_r (on heating), similar to

that shown in figure 4 (curve 3) and to that known from the literature [4, 11]. Furthermore, the maximum values of P_r are dependent on both the La content and the $F_{R(HT)}$–P_C phase transition temperatures (as shown in figure 2 for $\varepsilon(T)$ curves).

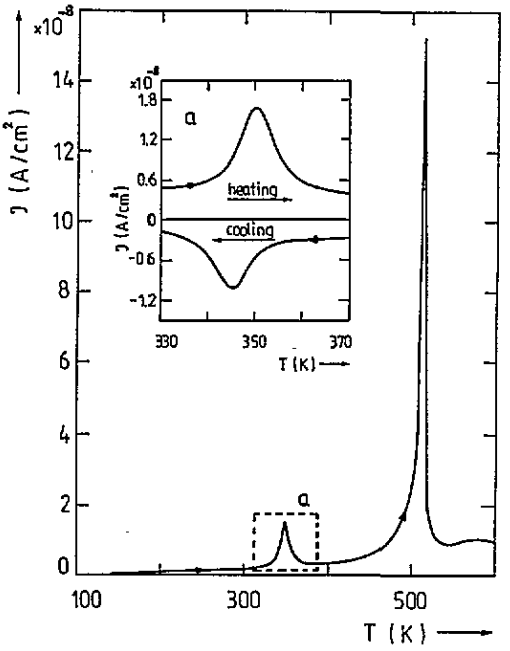

Figure 6. An example of the temperature dependence of the TSDC and pyroelectric current, measured on heating, for PLZT-92/8 + 0.4 at.% La ceramics. (a) The pyroelectric current measured on heating and on cooling through the $F_{R(LT)}$–$F_{R(HT)}$ phase transition.

Prior to pyroelectric measurements, the ceramic samples of 0.6 mm thickness were pre-polarized in a DC field of 5 kV cm^{-1} strength, applied for 30 min at 550 K, and during the subsequent cooling to 140 K. Then the samples were again heated at a rate of 5 K min^{-1} through all the above-mentioned phase transitions to about 600 K. An example of the recorded thermally stimulated depolarization current (TSDC) and the pyroelectric current is shown in figure 6. Pyroelectric current peaks on the background of TSDC appear in the vicinity of the $F_{R(LT)}$–$F_{R(HT)}$ and $F_{R(HT)}$–P_C phase transition temperatures. It is noteworthy that there is a distinct correlation between these pyroelectric current peaks and the anomalies in the dielectric characteristics discussed above (figures 2–5). The pyroelectric current associated with the A_O–$F_{R(LT)}$ phase transition was not observed, probably owing to the strongly diffuse nature of this phase transition. Its shift downwards, i.e. below the range in which the described measurements were performed, should also be taken into consideration. This shift could be caused by the prior pre-polarization, necessary for the pyroelectric measurements.

4. X-ray measurements

A PZT-92/8 ceramic disc sample of diameter 17 mm was used for x-ray experiments. Measurements were performed on a modified Dron diffractometer in a heating process using

Cu Kα radiation. Low-temperature (liquid-nitrogen) and high-temperature attachments were used, permitting temperature stabilization with an accuracy of ±0.5 K.

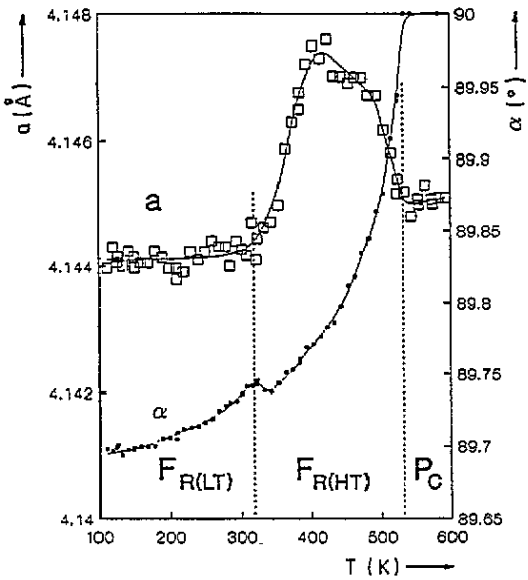

Figure 7. The parameters of the pseudoperovskite cell versus temperature for the PZT-92/8 ceramics.

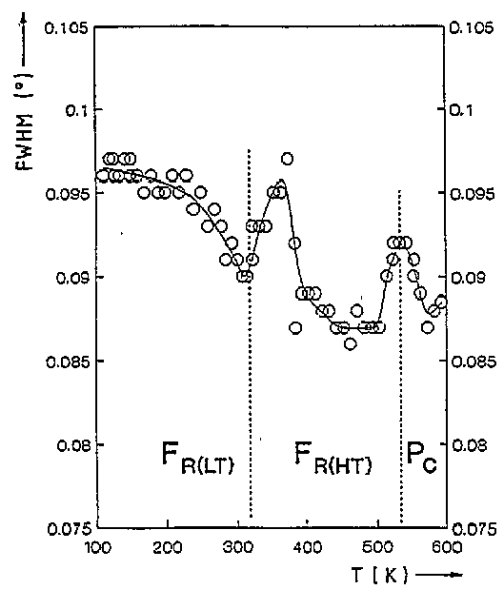

Figure 8. FWHM of the (200) line versus temperature for the PZT-92/8 ceramics.

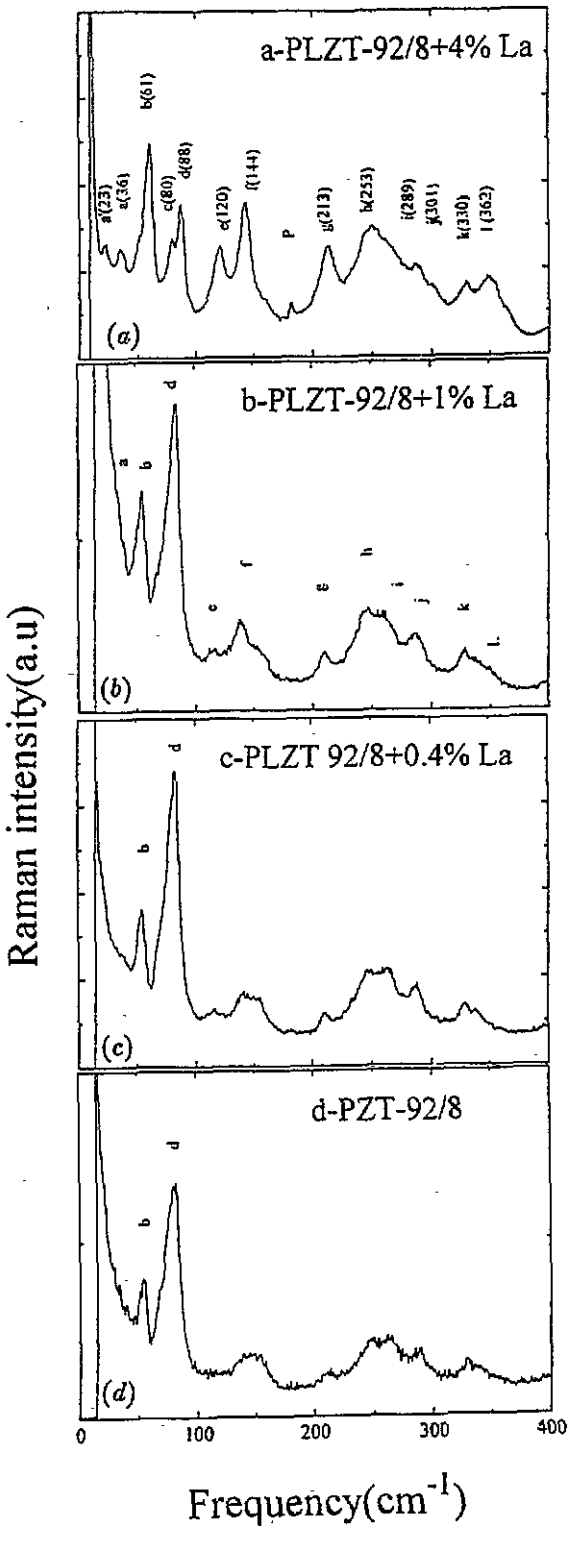

Figure 9. Comparison of Raman spectra at 10 K for (a) PLZT-92/8 + 4 at.% La (from [21]), (b) PLZT-92/8 + 1 at.% La, (c) PLZT-92/8 + 0.4 at.% La and (d) PZT-92/8 (a.u., arbitrary units).

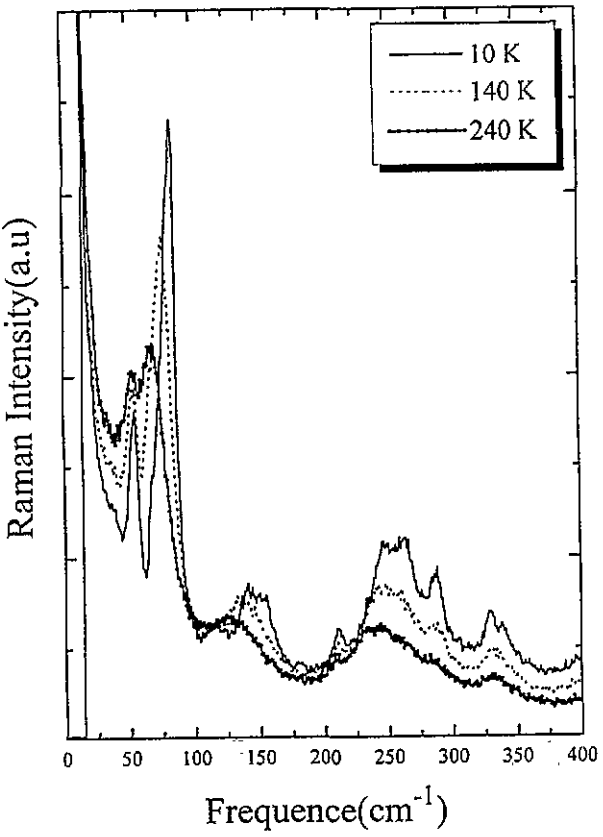

Figure 10. The temperature evolution of the Raman spectra in the vicinity of the A_O–$F_{R(LT)}$ phase transition for the PLZT-92/8 + 0.4 at.% La ceramics (a.u., arbitrary units).

The diffraction lines (200), (222) and (22$\bar{2}$) were studied to observe the changes in pseudoperovskite cell parameters (figure 7). Within the limits of the test temperature range, three different phases were found. The first, existing up to 340 K (low-temperature range), and the second, existing between 340 and 530 K (high-temperature range), had rhombohedral symmetry while the third, existing above 530 K, was cubic. As may be seen in figure 7, the boundaries between these phases are as follows: the step in temperature dependence of angle α, the point at which α becomes 90°, and the beginning and end of the convex part of the curve representing the temperature dependence of cell edge a. Moreover, in the vicinity of the temperatures of the phase transitions, maxima were observed on the temperature dependence of full width at half-maximum (FWHM) of the (200) line (figure 8). The difference between the symmetries of the low- and high-temperature rhombohedral phases was not determined.

The increase in the FWHM of the (200) diffraction line with decreasing temperature that can be observed below 300 K (figure 8) is unusual. Perhaps at low temperatures the line (200) is not the sole diffraction line. If this is so, the additional low-temperature phase with symmetry lower than rhombohedral (most probably an antiferroelectric phase of orthorhombic symmetry (A_O)) might coexist with the rhombohedral phase. Unfortunately, no evidence for the existence of such a phase was found within the experimental temperature range.

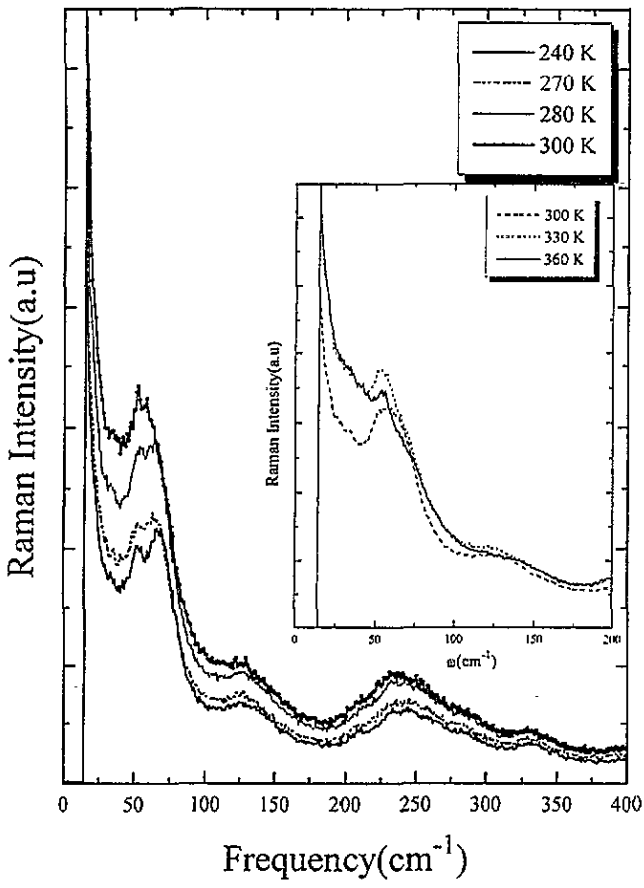

Figure 11. The temperature evolution of the Raman spectra around the $F_{R(LT)}$–$F_{R(HT)}$ phase transition for the PLZT-92/8 + 0.4 at.% La ceramics (a.u., arbitrary units).

5. Raman scattering measurements

Raman scattering measurements were carried out on a Spex double monochromator with a He–Ne laser (λ = 6328 Å) and an argon laser (λ = 5145 Å) using a photon-counting read-out system controlled by a Datamate acquisition processor. As previously mentioned, the partially transparent ceramics were suitable for use in 90° geometry Raman scattering measurements. The Raman spectra were recorded in a wide temperature range extending from 10 to 520 K. The low-temperature spectra were recorded on a sample cooled in an Air Product Displex crystal.

The Raman spectra recorded at 10 K for the investigated PZT-92/8, PLZT-92/8 + 0.4 at.% La and PLZT-92/8 + 1 at.% La ceramics are shown in figure 9. For comparison, Raman spectra for PLZT-92/8 + 4 at.% La from our recent paper [21] are also shown. As found in [21], the spectrum of the 4 at.% La-doped sample exhibits vibrational structures which are typical for the low-temperature antiferroelectric A_O phase, investigated by us for $PbZrO_3$ [24] and for the system PLZT-95/5 with La_2O_3 content up to 4 mol% [20]. On the other hand, Raman spectra for PZT-92/8, PLZT-92/8 + 0.4 at.% La and PLZT-92/8 + 1 at.% La exhibit differing characteristics which could be related, in line with previously presented

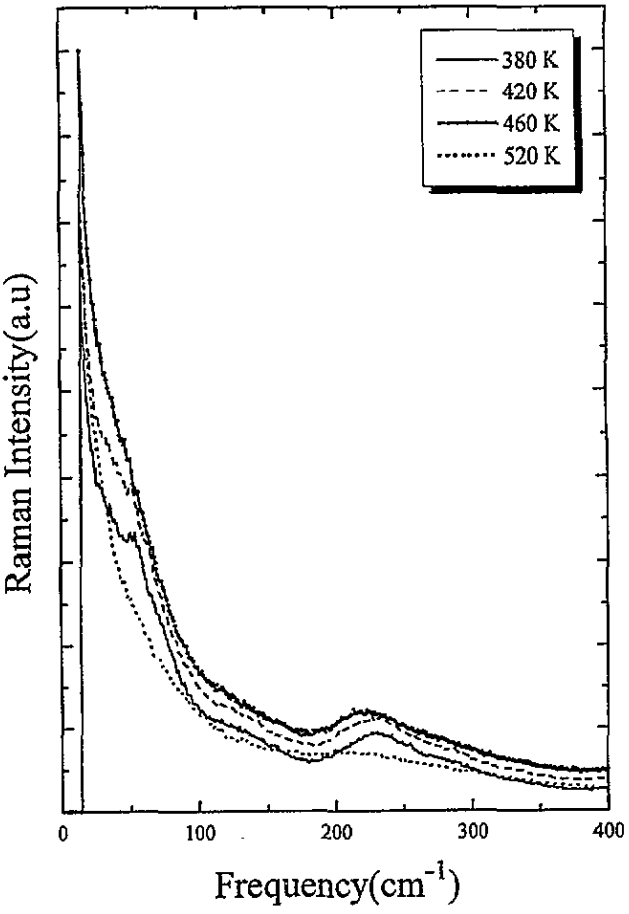

Figure 12. The temperature evolution of Raman spectra in the $F_{R(HT)}$ phase and in the vicinity of the $F_{R(HT)}$–P_C phase transition for the PLZT-92/8 + 0.4 at.% La ceramics (a.u., arbitrary units).

dielectric measurements to the occurrence of a low-temperature ferroelectric phase $F_{R(LT)}$. This probably results from a gradual shift in or even disappearance of the A_O phase with decrease in La content. However, at low temperatures the spectra recorded for both PLZT ceramics still exhibit a certain similarity to typical A_O phase forms.

The transformation of Raman spectra with temperature for PLZT-92/8 + 0.4 at.% La is shown in figures 10, 11 and 12. Data refer to the heating processes. The Raman spectra recorded up to $T < 200$ K are the most similar to the typical A_O phase spectra. All the spectra recorded at temperatures in the range from about 200 to about 330 K (figure 11) show certain common features, probably typical for the $F_{R(LT)}$ phase. The Raman spectra recorded at temepratures from about 360 to about 500 K (figure 12) are typical for the $F_{R(HT)}$ phase, ascertained earlier for the PLZT-95/5 + x at.% La system [20]. Traces of vibrational structures disappear when the $F_{R(HT)}$–P_C phase transition temeperature is reached (see the spectra recorded at 520 K).

The shifts in the mode frequencies and damping were systematically analysed by fitting Raman profiles to response functions, including a Debye-like function for the quasi-elastic scattering and a Lorentzian function for the resonant phonon scattering. Figure 13 presents

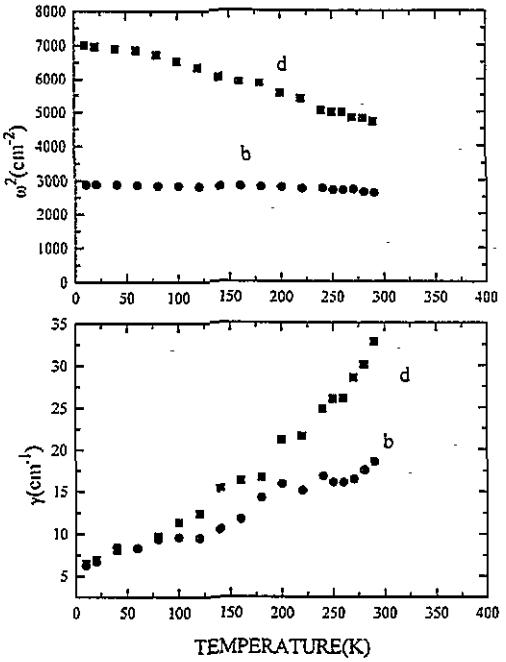

Figure 13. The squared freqency and damping factor (linewidth) of the b and d modes for PLZT-92/8 + 0.4 at.% La ceramics.

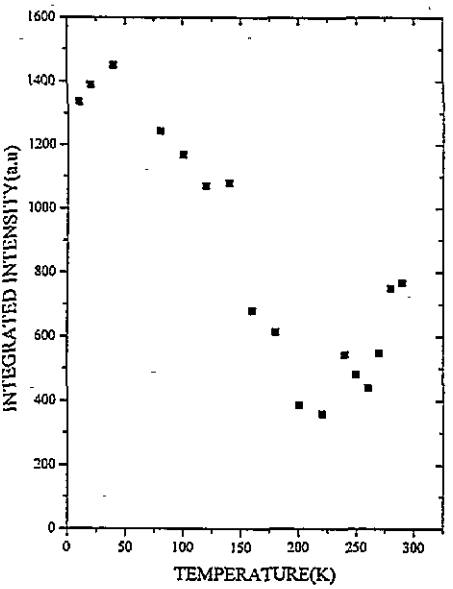

Figure 14. The integrated intensity versus temperature of the d mode for PLZT-92/8 + 0.4 at.% La ceramics (a.u., arbitrary units).

the deduced temperature dependence of the squared frequencies and the damping factor γ of modes b and d in figure 9. It may be observed that the $\omega^2(T)$ and $\gamma(T)$ curves exhibit relatively small changes when passing through the temperature range 200–240 K; these vibrational modes disappear when the $F_{R(LT)}$–$F_{R(HT)}$ phase transition temperature is reached on heating.

The presumed A_O–$F_{R(LT)}$ phase transition indicated for PLZT-92/8 + 0.4 at.% La and also by certain anomalies in dielectric characteristics (figures 3 and 4) is seen most significantly in the integrated intensity of mode d, showing a clear minimum in the vicinity of 200 K, as seen in figure 14.

More details of Raman scattering measurements performed for the PLZT-92/8 ceramics with La contents of up to 8 at.%, will be reported shortly in a separate paper.

6. Discussion

As mentioned in the introduction, the phase diagrams recently published for PZT and PLZT solid solutions [6, 7] show the occurrence of two ferroelectric phases of rhombohedral symmetry in Zr-rich PZT ceramics and only one in PLZT ceramics. This refers to ceramics of composition close to the phase boundary separating the A_O and F_R phases (figure 1).

Our measurements, carried out for PZT-92/8 ceramics, also indicate the occurrence of both a low-temperature ferroelectric phase $F_{R(LT)}$ and a high-temperature ferroelectric phase $F_{R(HT)}$. This was ascertained from all dielectric, pyroelectric and x-ray tests and confirmed by Raman scattering measurements. Even additional indications of the $F_{R(LT)}$–$F_{R(HT)}$ phase

transition were found, when comparing with earlier papers dealing with PZT ceramics with a Ti content of 6–12 at.% [8–17]. Certain details in the dielectric and x-ray measurements suggest that the occurrence of an A_O phase, and its coexistence with the $F_{R(LT)}$ phase in the low-temperature range in the PZT-92/8 ceramics also cannot be ruled out.

During recent investigations on PLZT ceramics with a Zr/Ti ratio of 92/8 and 4 at.% La (2 mol% La_2O_3) [21] we ascertained a strongly diffuse but direct A_O–$F_{R(HT)}$ phase transition. This is in agreement with the phase diagrams for PLZT materials reported earlier [5–7].

The results reported in the present paper for PLZT-92/8 ceramics with a La content up to 1 at.% showed, however, the occurrence of both $F_{R(LT)}$ and $F_{R(HT)}$ phases in these ceramics. On comparison of the results for PLZT ceramics with a ratio Zr/Ti of 92/8 and with various La contents, it may be confirmed that the low-temperature ferroelectric phase $F_{R(LT)}$ in PLZT-92/8 ceramics disappears at a certain La content in the range from 1 to 2 at.%. Symptoms of the $F_{R(LT)}$–$F_{R(HT)}$ phase transition were not found for the PLZT-92/8 + 2 at.% La ceramics whereas the PLZT-92/8 ceramics with a La content up to 1 at.% exhibit the A_O–$F_{R(LT)}$–$F_{R(HT)}$–P_C phase sequence. Certain features of the investigated characteristics seem to indicate that, with increasing La content, the A_O–$F_{R(LT)}$ phase transition temperature shifts towards higher temperatures (e.g. figure 5). As determined in our earlier paper [19], in the PLZT-95/5 + x at.% La ceramics the A_O–$F_{R(HT)}$ phase transition temperature shifts downwards with increase in La content. Both these shifts lead to a gradual narrowing of the $F_{R(LT)}$ phase, which at a given La content disappears entirely.

The results reported indicate that the phase diagram for the PLZT ceramics known from the literature [5–7] is incomplete since it does not take into account the presence of two different ferroelectric phases in the low-La-content region.

References

[1] Shirane G and Suzuki K 1952 *J. Phys. Soc. Japan* 7 333
[2] Sawaquchi E and Jaffe B 1953 *J. Phys. Soc. Japan* **8** 615
[3] Hańderek J and Ujma Z 1977 *Acta Phys. Pol.* A **51** 87
[4] Haun H I, Halemane T R, Newnham R E and Cross L E 1985 *Japan. J. Appl. Phys.* **24** 209
[5] Haertling G H and Land C E 1971 *J. Am. Ceram. Soc.* **54** 1
[6] Haertling G H 1987 *Ferroelectrics* **75** 25
[7] Haertling G H 1991 *Ceramic Materials for Electronics* (New York: Buchanan) ch 3
[8] Shirane G and Takeda A 1952 *J. Phys. Soc. Japan* 7 5
[9] Michel C, Moreau I M, Achenbach G D, Gerson R and Janes W I 1969 *Solid State Commun.* 7 865
[10] Clarke R and Glazer A M 1974 *J. Phys. C: Solid State Phys.* 7 2147
[11] Clarke R and Whatmore R W 1976 *J. Cryst. Growth* **33** 525
[12] Clarke R, Glazer A M, Aiger F W, Appleby D, Poole N J and Porter S G 1976 *Ferroelectrics* **11** 359
[13] Baüerle D, Holzapfel W B, Pinczuk A and Yacoby Y 1977 *Phys. Status Solidi* b **83** 99
[14] Whatmore R W, Clarke R and Glazer 1978 *J. Phys. C: Solid State Phys.* **11** 3089
[15] Glazer A M, Mabud S A and Clarke R 1978 *Acta Crystallogr.* B 34 1060
[16] Halemane T R, Haun H I, Cross L E and Newnham R E 1985 *Ferroelectrics* **62** 1159
[17] Randall C A, Matsko M G, Cao W and Bhalla A S 1993 *Solid State Commun.* **85** 193
[18] Fritz I J and Keck J D 1978 *J. Phys. Chem. Solids* **39** 1163
[19] Hańderek J, Ujma Z, Carabatos-Nedelec C, Kugel G E, Dmytrów D and El Harrad I 1993 *J. Appl. Phys.* **73** 367
[20] El Harrad I, Carabatos-Nedelec C, Hańderek J, Ujma Z and Dmytrów D 1994 *J. Raman Spectrosc.* **25** 799
[21] Ujma Z, Hańderek J, Hassan H, Kugel G E, Carabatos-Nedelec C and Pawełczyk M 1994 *J. Phys.: Condens. Matter* **6** 6843
[22] Kugel G E, Hafid M, Hańderek J, Ujma Z and Dmytrów D 1992 *Ferroelectrics* **133** 121
[23] Cross L E 1987 *Ferroelectrics* **76** 241
[24] Kugel G E, Lahlou S, Hańderek J, Ujma Z, Wójcik K, Roleder K, Fontana M D and Carabatos-Nedelec C 1990 *Ferroelectrics* **107** 103